AD-765 346

NONCRYSTALLINE SEMICONDUCTORS: ELECTRICAL AND THERMAL PROCESSES

Lyle H. Slack

Virginia Polytechnic Institute and State University

Prepared for:

Advanced Research Projects Agency

1 August 1973

Semiannual Technical Report

Title: Noncrystalline Semiconductors: Electrical and Thermal Processes

ARPA Order No. 1562, Amend No. 1

Grant No. DA-ARO-D-31-124-72-G72

Program Code No. 61101D

Principal Investigator and Project Scientist:

Lyle H. Slack
(703) 951-5600

Effective Date of Grant: 1 January 1972

Expiration Date: 31 December, 1973

Date of Report: August 1, 1973

Amount of Grant: $40,000

Semiannual Technical Report

AMORPHOUS SEMICONDUCTORS: ELECTRICAL AND THERMAL PROCESSES

Preface

Characterization of the switching processes in selected amorphous semiconductors continues to be the focus of this work. The work is progressing in two related channels, the first comparing the actual switching behavior of amorphous semiconductor films with computer simulations based on an assumed thermal model, and the second correlating the observed electronic spectra of crystalline and amorphous semiconductors with their electrical characteristics.

Two papers have been written during the past six months which are based on research funded by this grant. The first, coauthored by L. H. Slack and L. R. Durden and entitled "Observation of Electronic Spectra in Glass and Ceramic Surfaces" is being presented on August 27, 1973, at a conference "Surfaces and Interfaces of Glass and Ceramics" being held at Alfred University, Alfred, New York. The paper will be published by Plenum Press in the proceedings of the conference as a volume of their Materials Science Research Series. The second paper by W. D. Leahy, T. P. Kabaservice, and L. H. Slack will be presented by the principal investigator at the Fifth International Conference on Amorphous and Liquid Semiconductors, at Garmish-Partenkirchen, Germany on September 5, 1973. This paper will appear in the proceedings of the conference to be published in the Journal of Non-crystalline Solids.

1

Semiannual Rechnical Report

AMORPHOUS SEMICONDUCTORS: ELECTRICAL AND THERMAL PROCESSES

Part I

Experimental and Computer Studies of Switching in AsTe Films

A. Introduction

The study of switching has turned from the low melting chalcogenide glasses to the more stable semiconducting oxide glasses. Much of the past six months has been spent in learning to make ceramic sputtering targets which would not fracture during radio frequency sputtering, and to sputter oxide thin films. The oxides studied are from the V_2O_5 - P_2O_5 system and some selected compositions with the major component being Bi_2O_3.

The V_2O_5 - P_2O_5 system was chosen because the system has been characterized in the literature[1-12] and is known to give a variation in conductivity. The Bi_2O_3 compositions are of interest because switching has been observed in polycrystine ZnO containing Bi_2O_3[13,14]. Morris[15] has shown that this mixture sinters to a dense solid by liquid grain boundary sintering. He isolated the grain boundary phase by dissolving away the ZnO crystals with a preferential etchant. Electron microprobe analysis indicated that the Bi:Zn ratio in the grain boundary phase was between 10:1 and 3:1. The Bi_2O_3 - ZnO phase diagram[16] reveals that there is a 750°C eutectic at about 8 mole % ZnO, and that a G.c.c. phase forms containing about 11 mole % ZnO. The liquid phase that forms during sintering would have the eutectic composition, and would therefore be near the 10:1 Bi:Zn end of the range that Morris specified. The composition 86 Bi_2O_3:14 ZnO was chosen for thin film preparation and subsequent switching studies.

It is postulated that electrical conduction in this Bi_2O_3 - ZnO amorphous semiconductor phase is related to the multiple valence nature of the bismuth ion. MnO is another phase which has been found[17] to exhibit appreciable conduction. In an effort to enhance the conductivity of the Bi_2O_3 - ZnO phase, MnO was added. After consideration of the Bi_2O_3 - ZnO and Bi_2O_3 - MnO[8] phase diagrams, it was estimated that the eutectic in the Bi_2O_3:ZnO:MnO ternary system would at an approximate molar ratio of 70:10:20. This composition was also chosen for film preparation and switching studies. An approximate eutectic composition was chosen in order to facilitate fabrication of the sputtering target.

B. Preparation of V_2O_5 - P_2O_5 Glasses (written by M. Chakraborty)

Several attempts were made to form V_2O_5 - P_2O_5 glasses. The several techniques required using V_2O_5, 5N purity, as one starting compound and phosphorous pentoxide powder, P_2O_5, ammonium dihydrogen phosphate, $NH_4H_2PO_4$, or orthophospheric acid, H_3PO_4, as the additional compound.

The hydroscopic nature of P_2O_5 powder requires that all weighing operations and mixing be carried out in a dry nitrogen atmosphere. Initially the starting materials, V_2O_5 and P_2O_5, were placed in a Vycor tube and sealed under vacuum. However, slight exposure to atmospheric air, between the dry box and the vacuum pump, allowed the P_2O_5 to absorb moisture. Consequently, the mixture tended to foam rather than melt, causing the sealed tubes to explode. As a result this procedure was abandoned.

An alternative method was selected which required the thermal decomposition of $NH_4H_2PO_4$ to obtain P_2O_5 indirectly. The violence of the thermal decomposition of $NH_4H_2PO_4$ is sufficient to cause considerable loss of starting material resulting in a deviation in glass composition. This method was also abandoned.

A third method, which proved successful, required the decomposition of orthophosphoric acid to P_2O_5. Starting materials were placed in a beaker, with sufficient distilled water to form a slurry, then agitated for one half hour. The slurry was dried in an oven at 170°-175°C until it attained a constant weight (approx. 40 hours). The mixture appeared to have reacted chemically and the resultant product showed no tendency to pick up moisture from the atmosphere.

Reacted materials were melted in alumina crucibles with lids for one half hour. The molten liquid was poured onto a steel plate, which had been heated to 250°C, annealed at 270°C for eight hours and allowed to furnace cool. Final shaping of the glass samples, as R. F. Sputtering targets and thermal conductivity samples, was accomplished by grinding and polishing with silicon carbide.

C. Preparation of 86 $Bi_2O_3 \cdot 14$ ZnO and 70 $Bi_2O_3 \cdot 10ZnO:20$ MnO Films (written by W. D. Leahy)

Ceramic bodies for R. F. Sputtering and thermal conductivity measurements were prepared from analytical grade Bi_2O_3, ZnO, and MnO_2. Appropriate batches (~100 gms) were weighed on an analytical balance and mixed under acetone. After drying, 1-2% dextrin, by weight, was dry mixed into the batches followed by one drop of distilled water for every ten grams of batch. Sputtering targets and thermal conductivity samples were pressed at 10,000 pounds in $1\frac{1}{4}$ inch and 18 mm pellet presses respectively. All samples were fired at 700°C from four to twelve hours. For thermal conductivity, the pellets were ground smooth, after firing, on 600 grit silicon carbide paper to insure good thermal contact.

Sputtering targets were silver epoxied onto brass holders and resistor cement was applied around the base of the brass holder for extra mechanical strength.

Two types of substrates were used during sputtering, depending on the application. For electrical conductivity, glass slides masked with aluminum foil were used. The masking provided a step for the thickness measurement. For switching experiments, films were sputtered onto aluminum disks approximately 1 inch in diameter. V_2O_5 - P_2O_5 glasses were sputtered in argon. The bismuth oxide compositions required pure oxygen to eliminate reduction.

D. Electrical and Thermal Measurements on Oxide Films

At this writing, the oxide films have been deposited and the switching devices have been fabricated. Preliminary switching tests on a curve-tracer oscilloscope indicate that the $V_2O_5 \cdot P_2O_5$ film does demonstrate switching. The other oxide films require very high voltages.

Four point probe measurements of resistivity and thermal activation energy for conduction are in process. Thermal conductivity and heat capacity measurements are being carried out on the bulk V_2O_5 - P_2O_5 glasses and on the Bi_2O_3 - ZnO and Bi_2O_3 - ZnO - MnO ceramics, identical to the ones used for the sputtering targets.

When these physical property measurements are complete, the computer simulation of switching can proceed.

Part II

Electron Spectra of Selected Amorphous and Crystalline
Chalcogenide Alloys (written by L. R. Durden)

Several investigators[18,19] have shown experimentally that the optical and electrical properties of crystalline materials and amorphous films of the same compositions are quite different. Other investigators[20,21] have shown the value of X-ray photoelectron spectroscopy as a tool for studying the bonding characteristics of materials. The changes in the binding energy of the electrons and the shapes of occupied electron levels reveal the nature of the chemical bond. Shifts in binding energy vary in magnitude, with the particular level under investigation, with the relative electronegativity of the bonded elements and with the atomic structure of the solid. It is generally known, from band theory, that the valence electrons participate in bonding as well as conduction processes. Hence, it was proposed that spectroscopic studies, revealing the nature of the valence band, should yield some insight into the nature of the bond and the conduction process.

To date, selected subvalence and valence level X-ray photoelectron spectra have been collected for both polycrystalline samples and amorphous films of the following compositions: Ge, Si, C, Te, Se, $Ge_{40}Te_{60}$, GeTe, $Ge_{60}Te_{40}$, $GeSe_2$, $Ge_{43.5}Se_{56.5}$, and GeSe. These spectra, gathered using $AlK\alpha_{1,2}$ as an exciting source, and electrical conductivity data, where obtainable, are presented in this paper.

Sample Preparation

Samples of $Ge_{40}Te_{60}$, GeTe, $Se_{60}Te_{40}$, $GeSe_2$, $Ge_{43.5}Se_{56.5}$, and GeSe were prepared from elements whose purity was 99.99+% and semiconductor grade Si and Ge. Starting materials were placed in 22mm I.D. Vycor tubing, sealed under vacuum, and reacted for 72 hours with intermittent agitation.

All crystalline materials were water quenched to retain a fine grain structure.

Cylindrical wafers 0.5mm and 0.25 in. thick were sliced from the crystalline material and laminated, with electrically and thermally conducting silver epoxy, to holders suitable for insertion into the electron spectrometer[*] and the R. F. sputtering unit[**] respectively.

Amorphous thin films for electron spectroscopy and conductivity measurements were R. F. Sputtered directly onto suitable sample holders and glass microscope slides, respectively. In all cases thin film samples were prepared just prior to measurements and the collection of spectral data.

Data Collection

Electron spectral data included the range from the fermi level to 18 eV of binding energy as well as 5 eV of binding energy above and below the strongest subvalence level. The variable parameters of the spectrometer were selected to yield a resolution of not less than 0.1 eV.

Electrical conductivity measurements were made using the four-point probe technique as described by Valdes[22]. An environmental chamber[*3] was used to control the temperature, to within $1^{o}C$ of various set points, and the current and voltage were measured to a precision of not less than 3% using an electrometer and a microvolt-ammeter[*4] yielding a maximum probable error of 6%.

---

[*] AEI Scientific Apparatus limited. ES-100

[**] R. D. Mathis Co.

[3*] Delta Design, Inc., HK-2300, Temperature chamber

[4*] Kiethley Instruments, Inc., Model 153, Microvolt-ammeter
Kiethley Instruments, Inc., Model 610B, Multi-range electrometer.

Results

The valence level spectra of an amorphous film, prepared by electron beam evaporation, and crystalline Ge, Figure 1, show a well defined peak for the crystalline material at 3.0 eV that is absent in the amorphous material. To ascertain whether the absence of a well defined Ge 4p level was the result of the method of deposition, a similar film was prepared by R. F. sputtering, Figure 2. It is seen that the two spectra are identical in shape indicating that the mode of deposition did not distort the electron spectra.

Similar spectra collected for Si, Figure 3, show the same essential features as those for Ge. However, the prominent Si 3p level evident at 3.3 eV of binding energy in the crystalline sample is absent in both amorphous films. The structure, centered at 8.4 eV of binding energy, that is present in the sputtered film and absent in the vapor deposited film, is probably due to the occurrence of the S-like levels centered at 6.6 eV and 9.2 eV that have been reported by Ley et. al.[23] and could indicate some degree of ordering in the film. However, electron diffraction failed to indicate the presence of any micro-crystallites.

To ascertain whether the back streaming of carbon from diffusion pump oil could alter the valence level spectra a sputtered film of amorphous carbon was examined, Figure 4. There is no indication of any valence level structure in the energy range under study, leading to the conclusion that there is no significant contribution to valence level electron spectra from carbon contamination.

Valence band spectra of amorphous and crystalline $Ge_{40}Te_{60}$, GeTe, and $Ge_{60}Te_{40}$ are contained in Figures 5-7. Amorphous valence levels show a
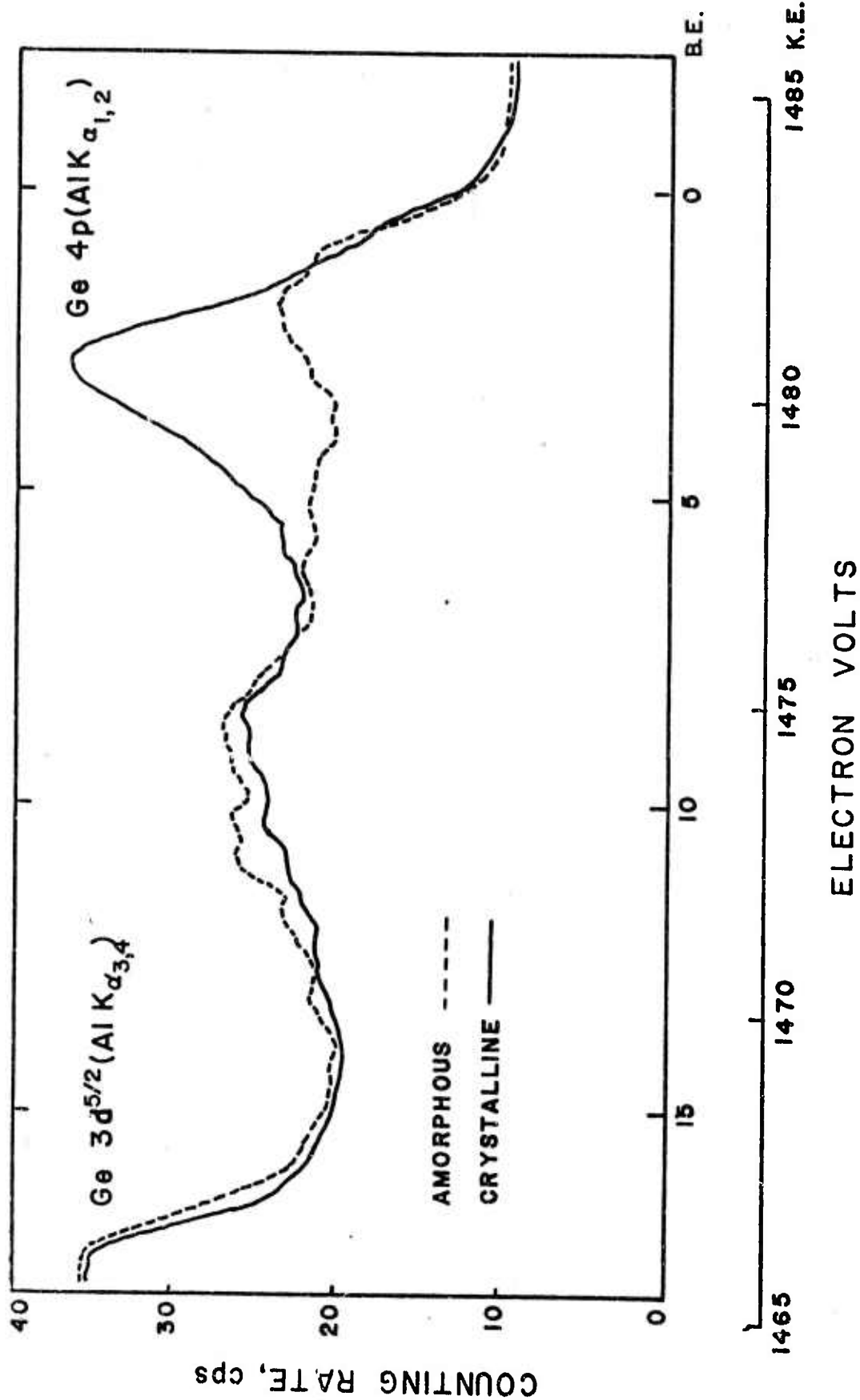
Figure 1. Valence levels of Amorphous, vapor deposited, and crystalline germanium.
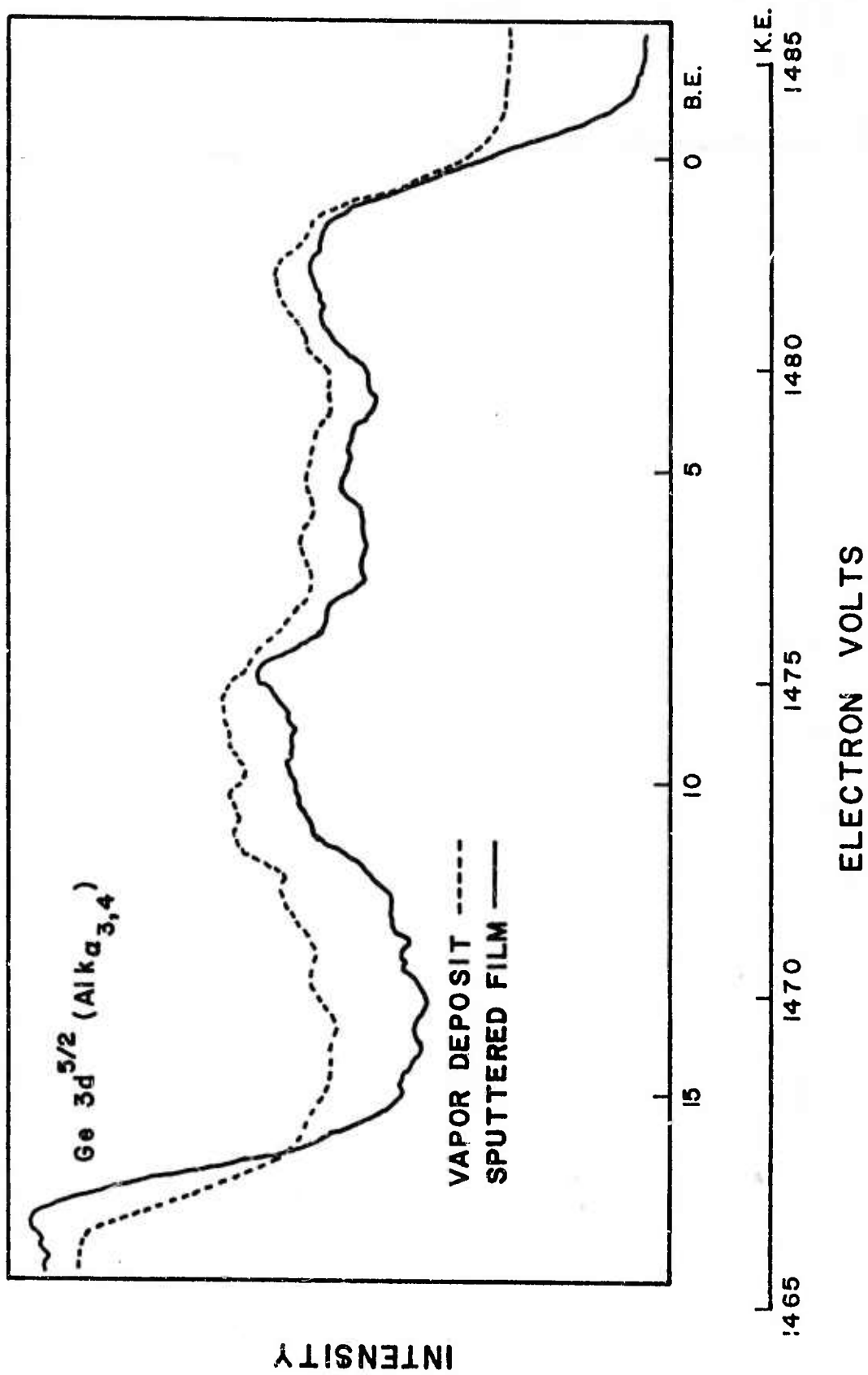
Figure 2. Comparison of the valence levels in vapor deposited and R.F. supttered Amorphous germanium films.
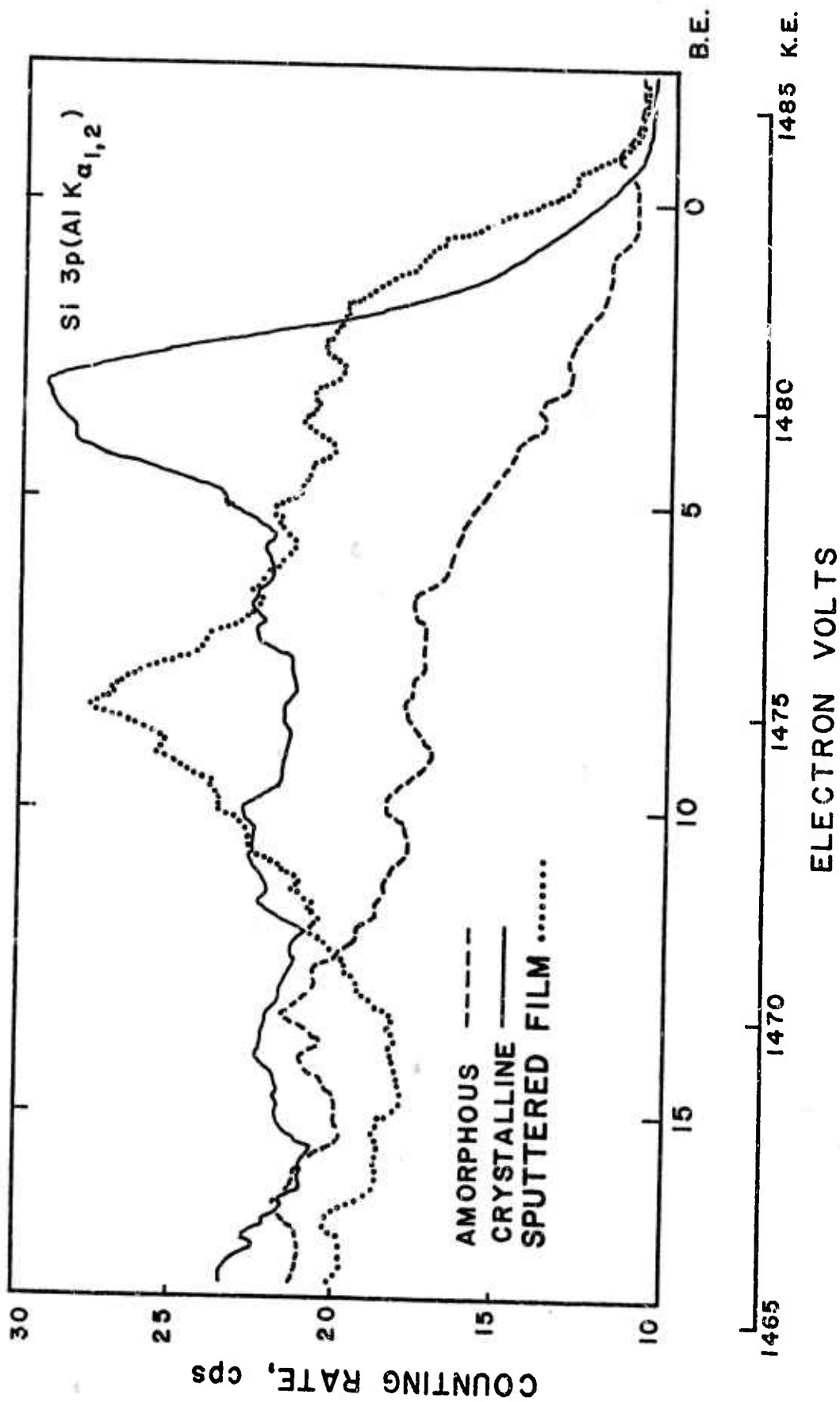
Figure 3. A comparison of the valence levels in crystalline silicon and amorphus silicon films that were produced by vapor deposition and R.F. sputtering.
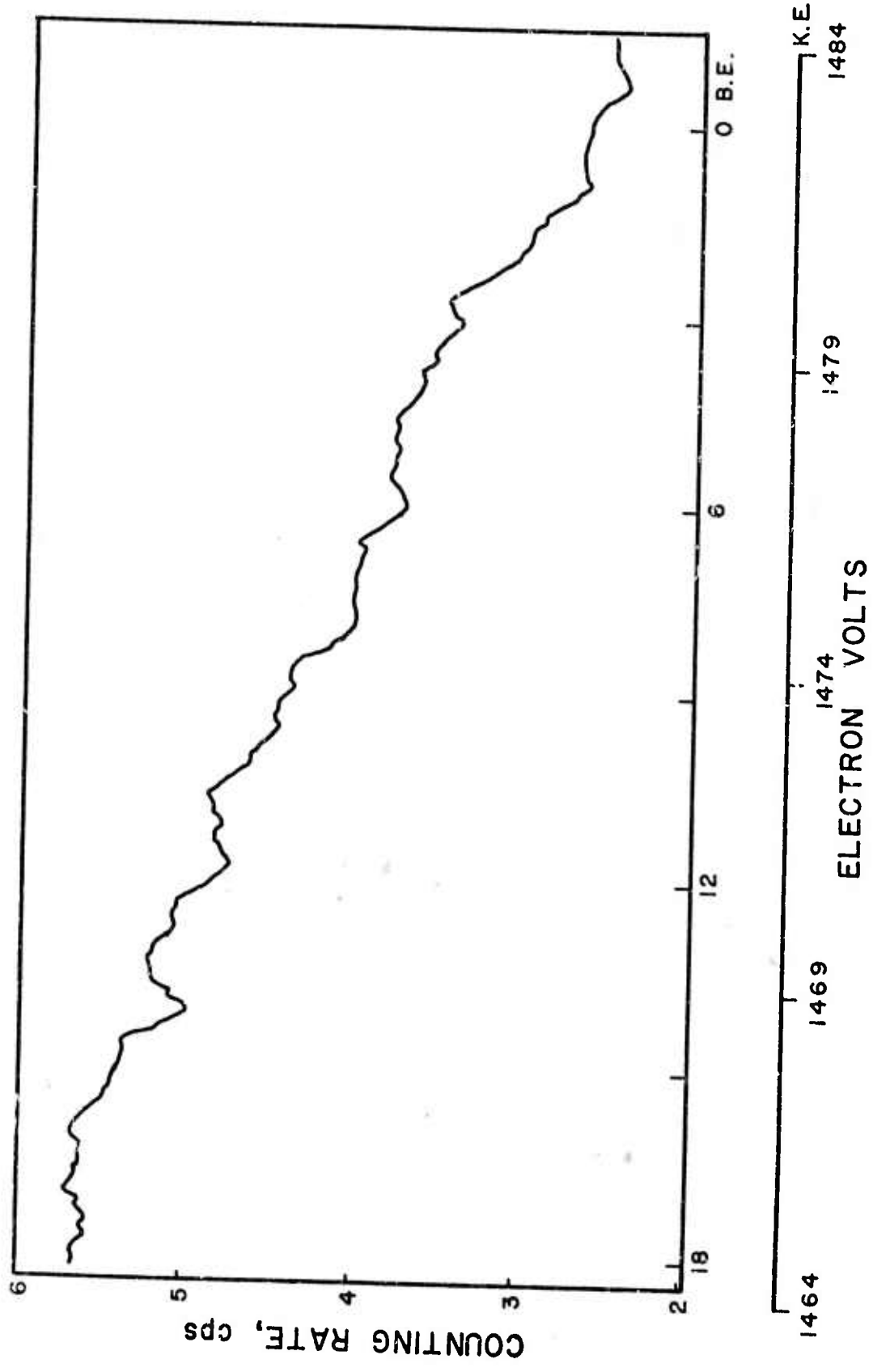
Figure 4. Valence levels in a sputtered carbon thin film.
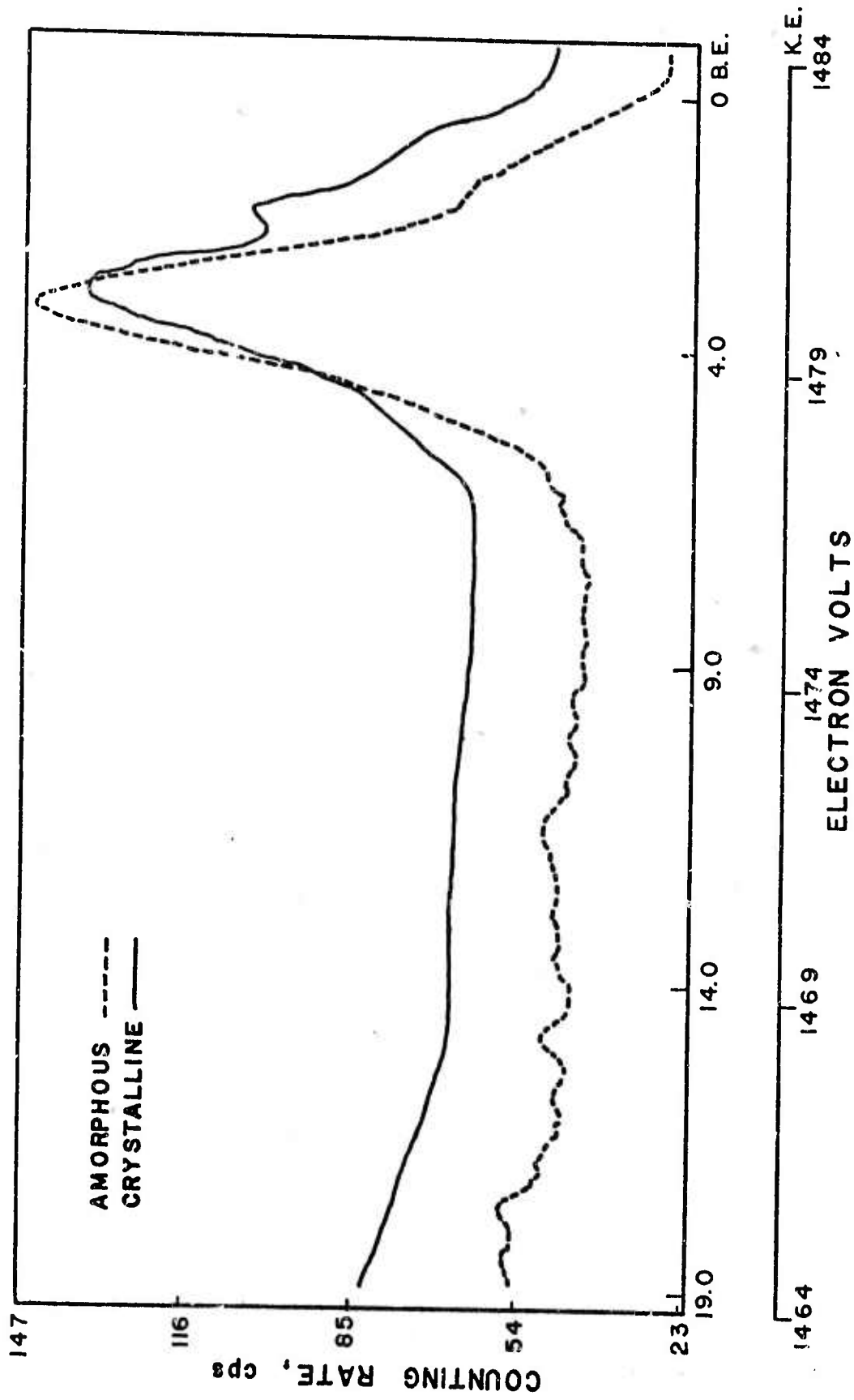
Figure 5. The outer electron levels of amorphous and crystalline $Ge_{40}Te_{60}$.
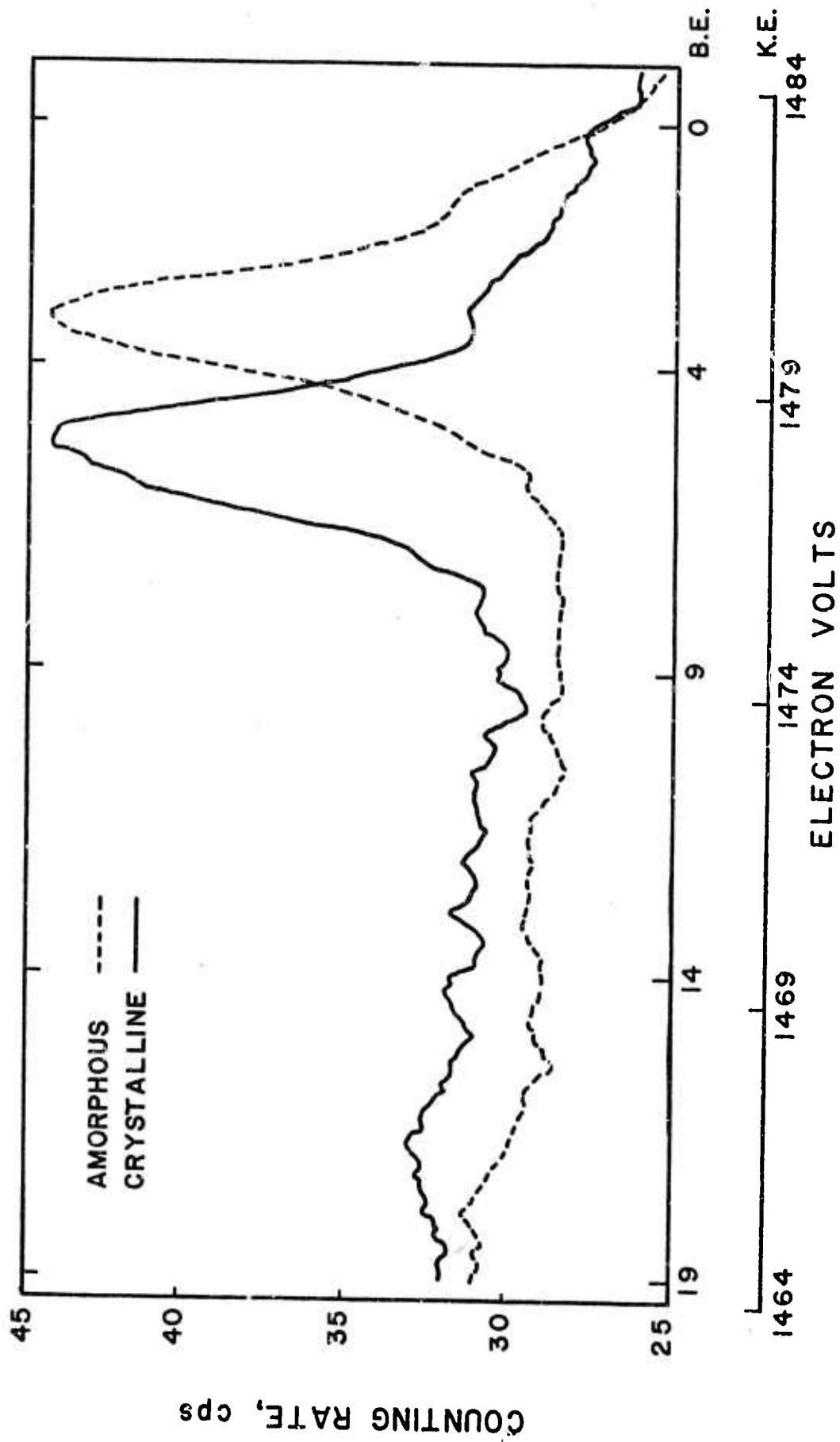
Figure 6. A comparison of the valence levels of amorphous and crystalline GeTe.
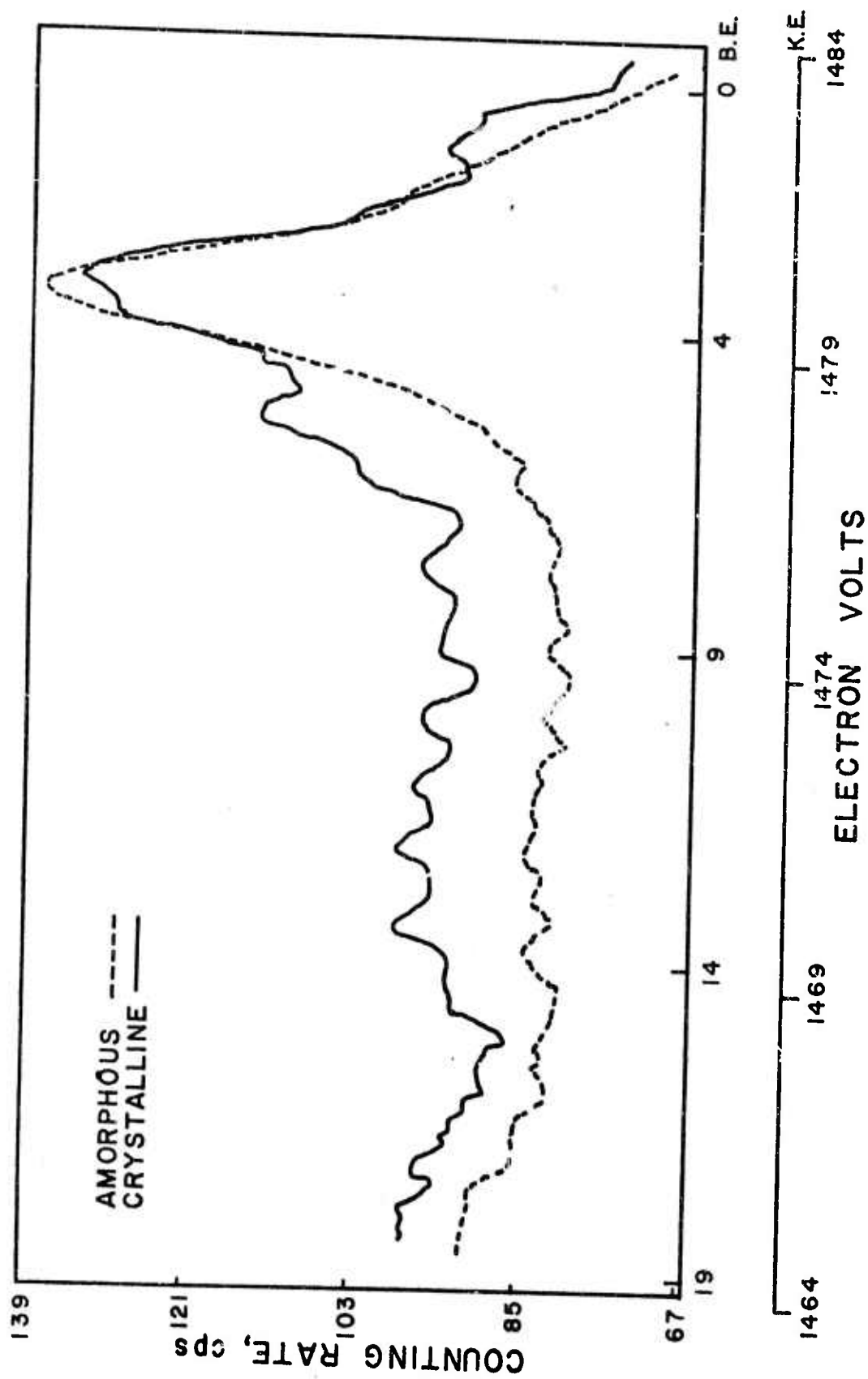
Figure 7. Valence level spectra of amorphous and crystalline $Ge_{60}Te_{40}$.

well d ined peak structure at 3.5 eV, 3.2 eV, and 3.4 eV respectively, while the crystalline valence levels have peaks at 3.2 eV and 1.8 eV, 5.3 eV, 5.3 eV and 3.4 eV respectively.

To aid in the identification of the valence level peaks in the spectra of the $Ge_x Te_{1-x}$ compositions, a valence level spectrum of polycrystalline Te was collected, Figure 8. The valence band of crystalline Te is shown at 2.2 eV. Comparison of the valence level in polycrystalline Ge, Figure 1, and in polycrystalline Te, Figure 8, with the valence electron levels of the $Ge_x Te_{1-x}$ compositions, shows that there is little similarity.

The valence electron level spectra of amorphous and polycrystalline $GeSe_2$, $Ge_{43.5} Se_{56.5}$ and GeSe, Figures 9-11, show several distinct differences. For the $GeSe_2$ and GeSe samples, the valence level spectra of the polycrystalline samples are quite broad when compared with the amorphous spectra, which have sharp, well defined peaks at 2.5 eV of binding energy. The crystalline valence levels of $Ge_{43.5} Se_{56.5}$ are quite well defined compared to those of $GeSe_2$ and GeSe. Amorphous valence electron levels of $Ge_{43.5} Se_{56.5}$ are quite well defined and clearly show an s-like doublet at 9.5 eV and 8.1 eV of binding energy with only a remnant of the crystalline levels present.

Elemental Se, Figure 12, has a well defined valence level spectrum with peaks at 6.2 eV and 3.2 eV of binding energy, that compare to the 4p electron levels. Considering the appropriate valence level shifts, relating to atomic bonding, when Ge, Figure 1, and Se, Figure 11, are combined, could account for the broad crystalline peaks found in the $Ge_x Se_{1-x}$ samples.

Amorphous and polycrystalline AsTe, Figure 13, have valence levels that resemble those of $Ge_{43.5} Se_{56.5}$. The polycrystalline sample shows a skewed peak beginning at 7.3 eV and ending near zero eV with its center
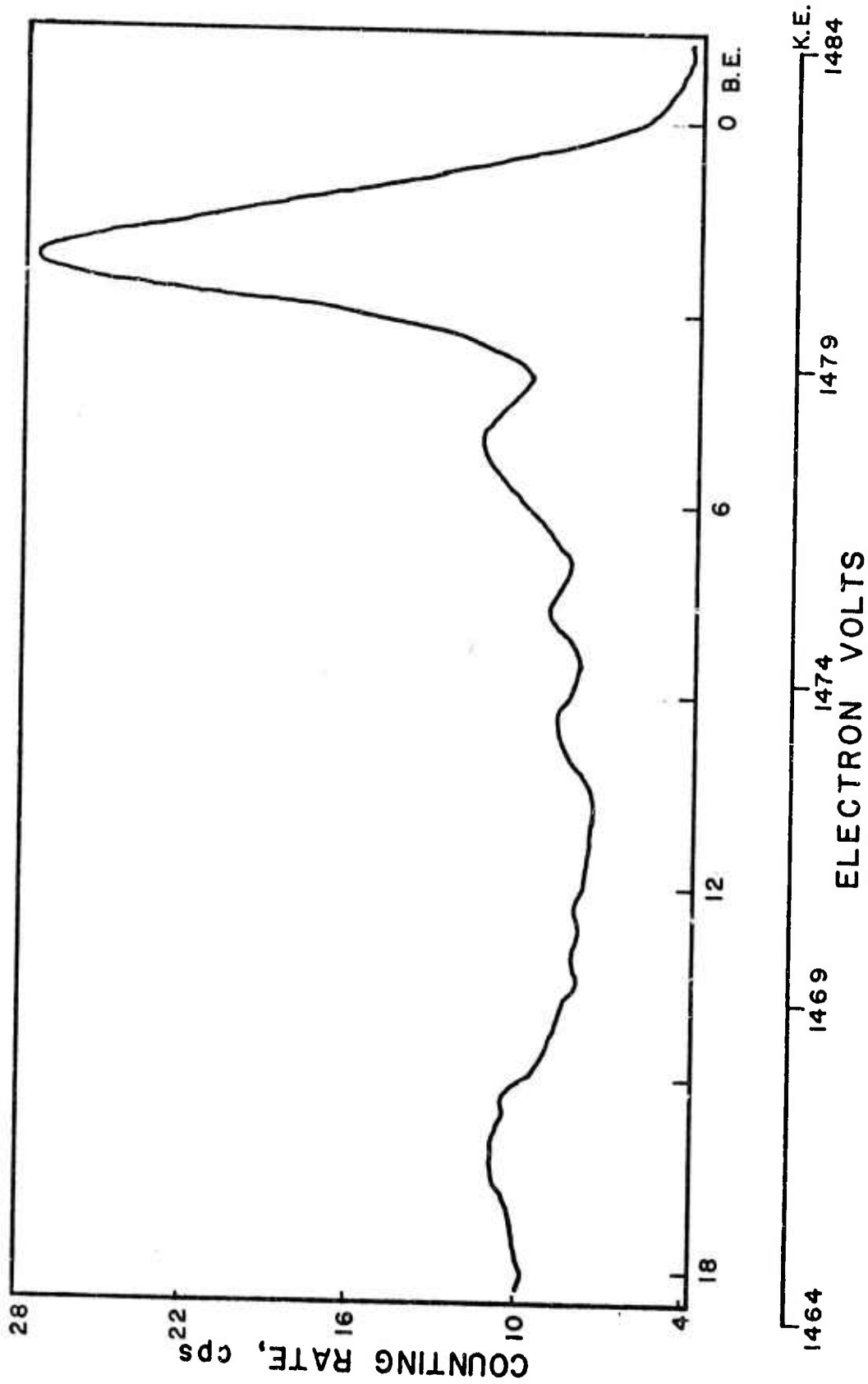
Figure 8. The tellurium 5p levels from a polycrystalline sample.

18
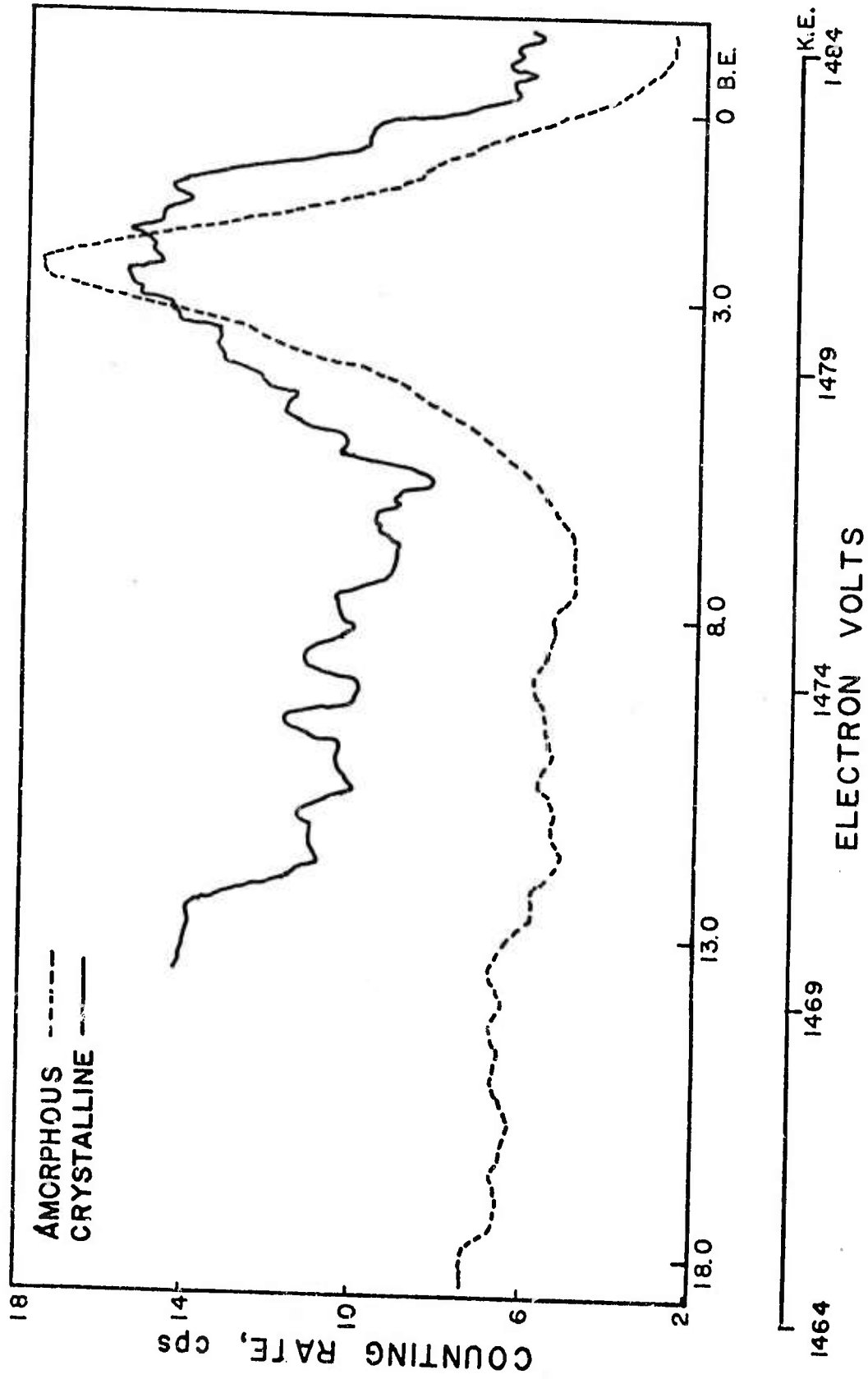
Figure 9. The outer level spectra of amorphous and crystalline $GeSe_2$.
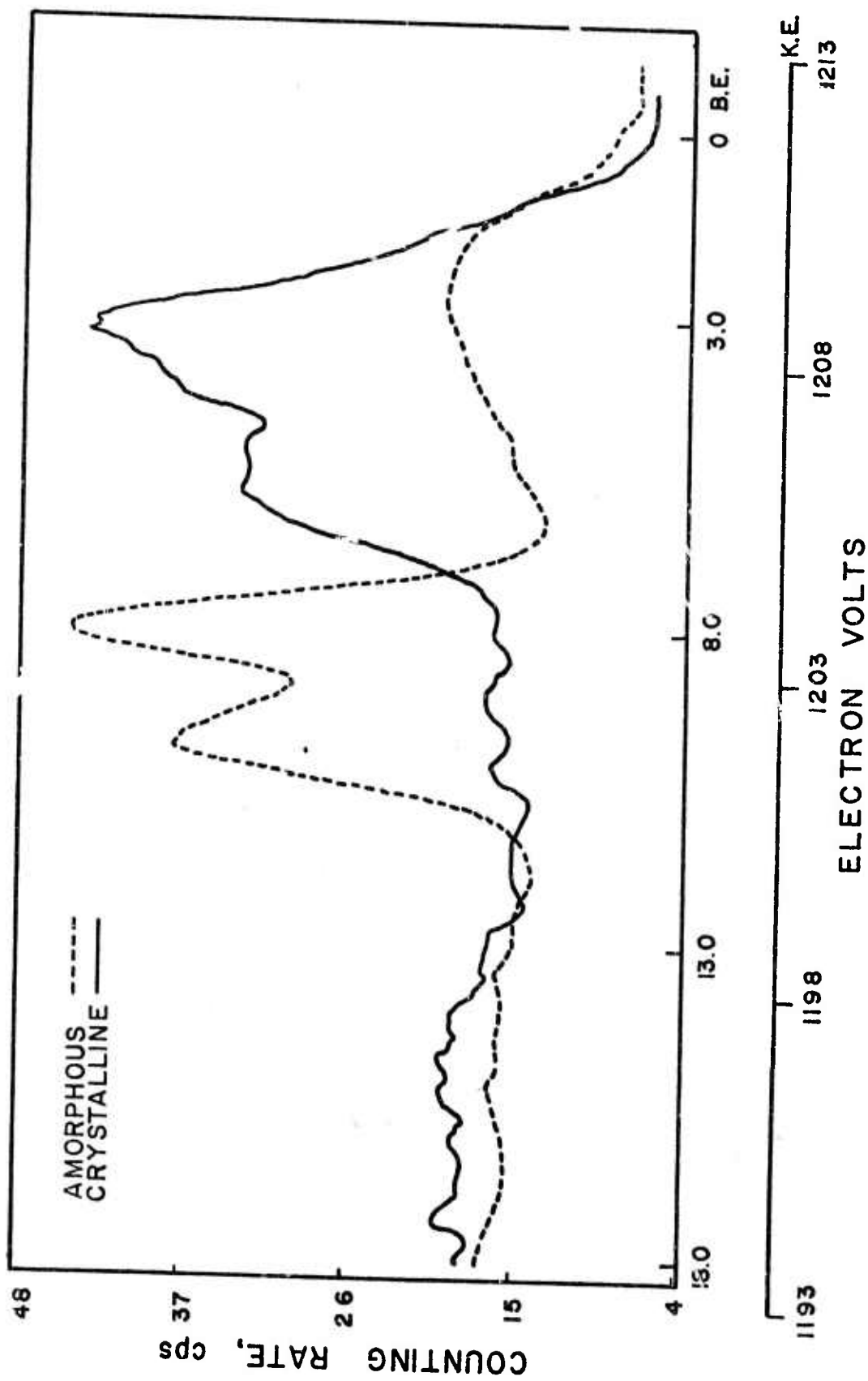
Figure 10. Valence level spectra of amorphous and crystalline Ge$_{43.5}$Se$_{56.5}$.
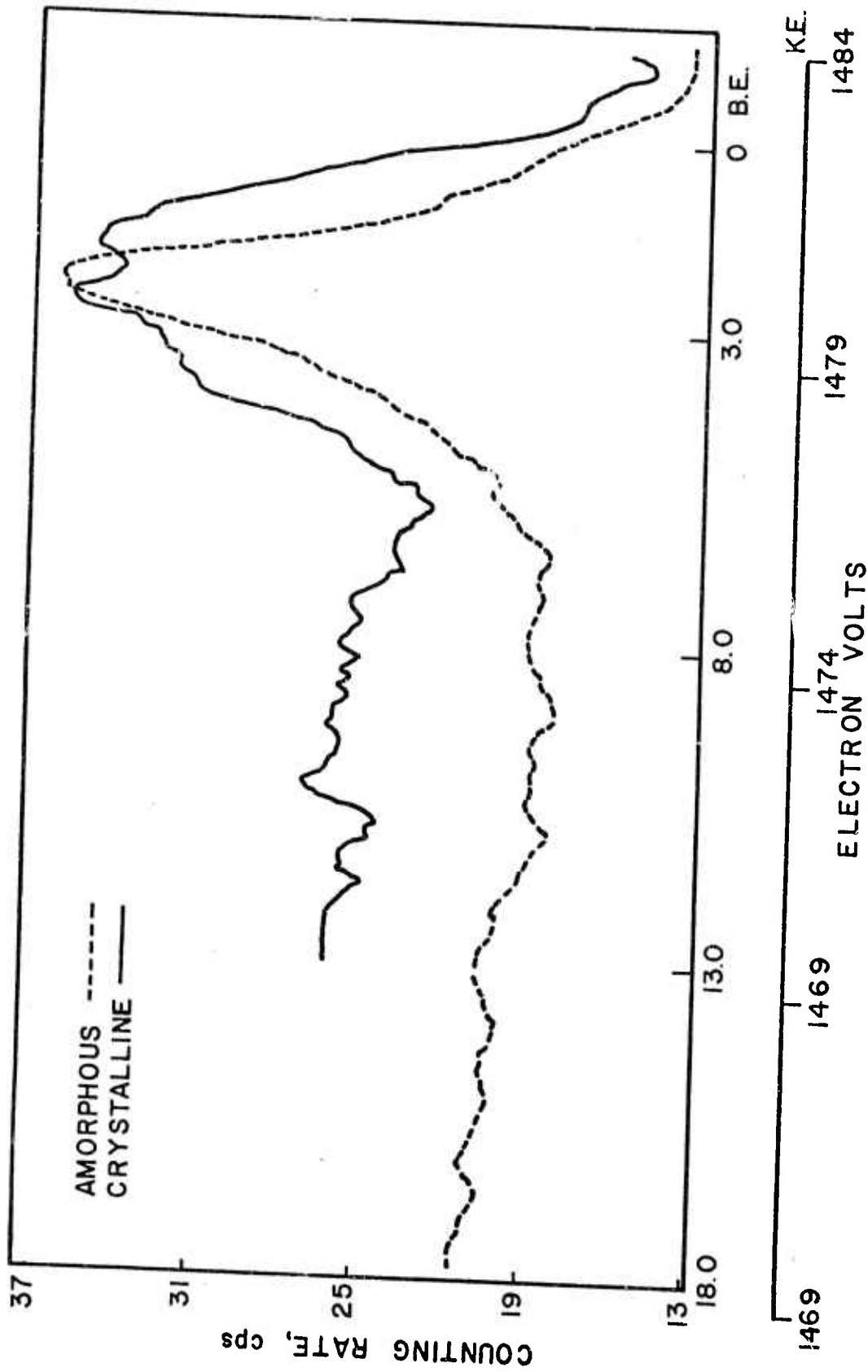
Figure 11. A comparison of the valence level spectrum of amorphous and crystalline GeSe.
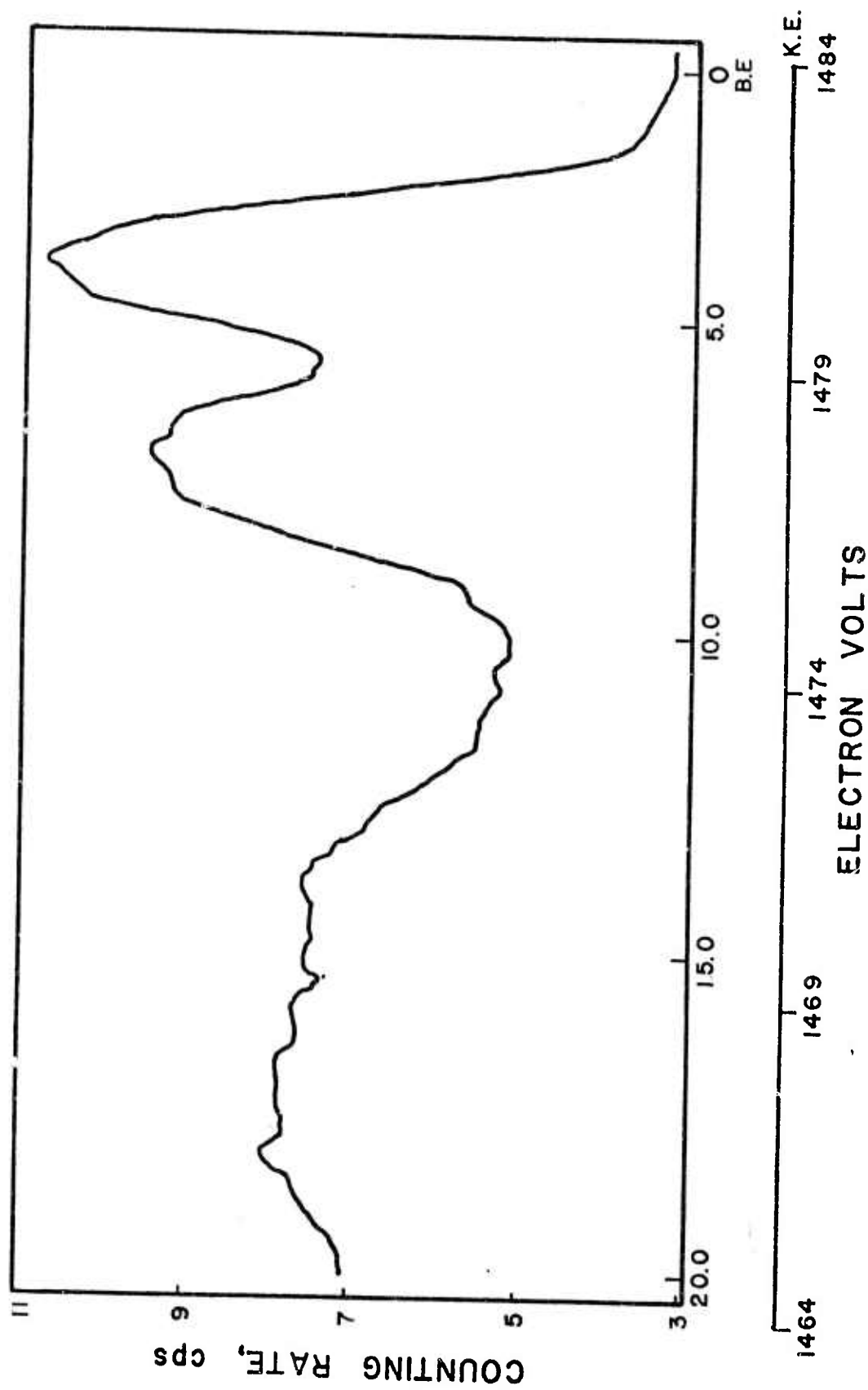
Figure 12. Valence levels in amorphous selenium.
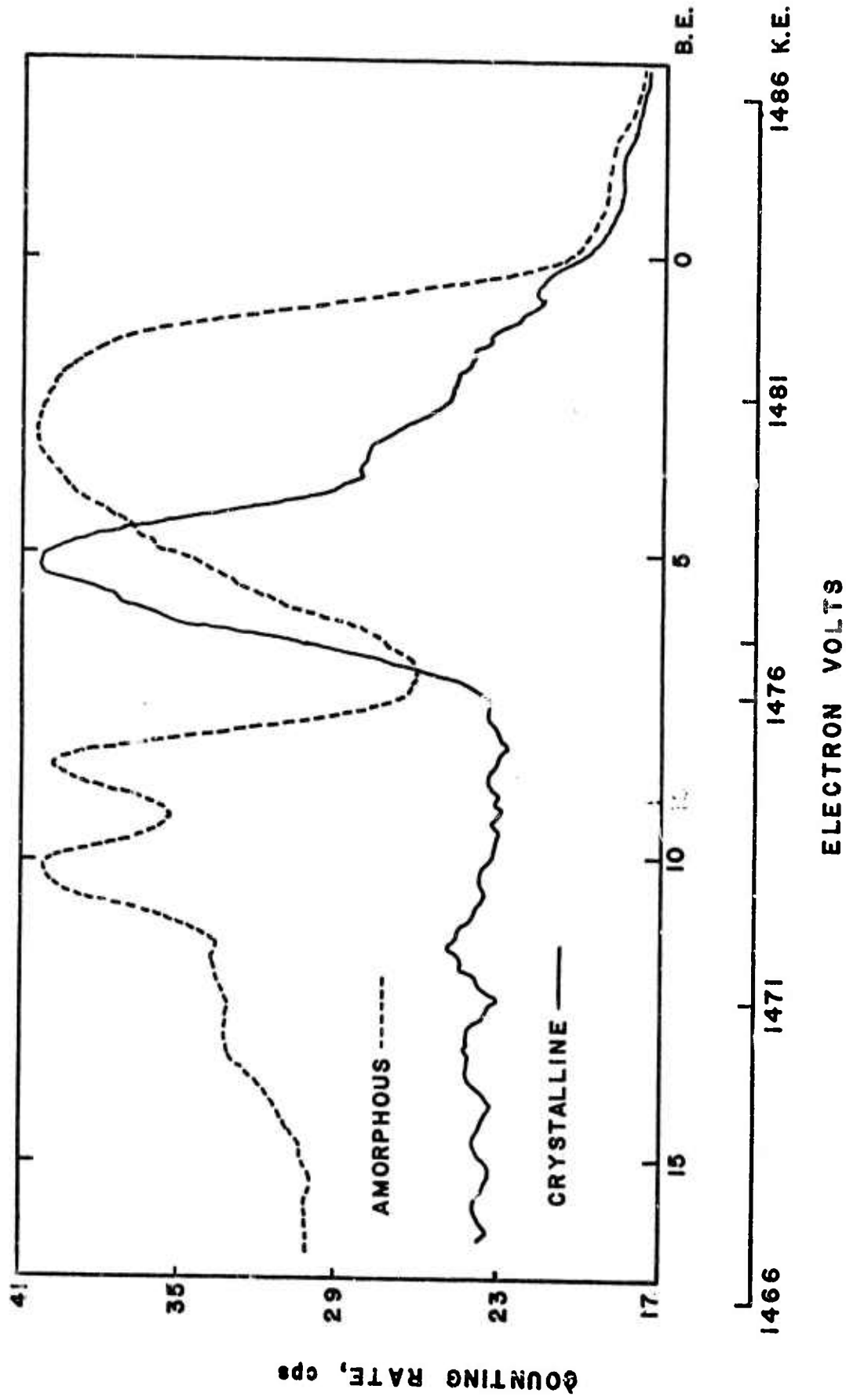
Figure 13. Valence level spectra of amorphous and crystalline AsTe.

at 5.2 eV. The amorphous spectrum contains three peaks, two that are part of a doublet at 10.0 eV and 8.5 eV, and a broad peak extending from 15.8 eV to zero eV with its center at 2.9 eV.

Comparison of the binding energy of the strongest subvalence level of each element among the polycrystalline elements, polycrystalline alloys and amorphous films, failed to show any evidence of peak shifts, or half height peak broadening, that could be associated with changes in atomic bonding or coordination.

Variation of the electrical conductivity of amorphous and crystalline Ge_xTe_{1-x} compositions and selected elements, Figures 14 and 15, show that generally the crystalline materials are several orders of magnitude more conducting than amorphous materials of the same composition. This fact alone indicates that there is some electronic and structural difference that tends to reduce the mobility of charge carriers in amorphous materials. The precise mechanism is yet to be determined.

Discussion

The electronic structure of fourth period metalloids is such that the valence electron levels, a combination of s and p orbitals, overlap to form an sp^3 hybridized band that gives rise to tetrahedral coordination. At true crystallographic equilibrium the sp band splits into two bands, the lower energy, valence band, being completely filled and the upper energy band, conduction band, being completely empty[24]. The fermi level lies between the valence and conduction bands. Since it is not likely that that structural disorder could broaden energy levels by several eV, it is concluded that the valence level structure is distorted due to trapping of electrons in high energy traps, that result from structural disorder and unsatisfied bonds. Such an explanation would also explain the reduction
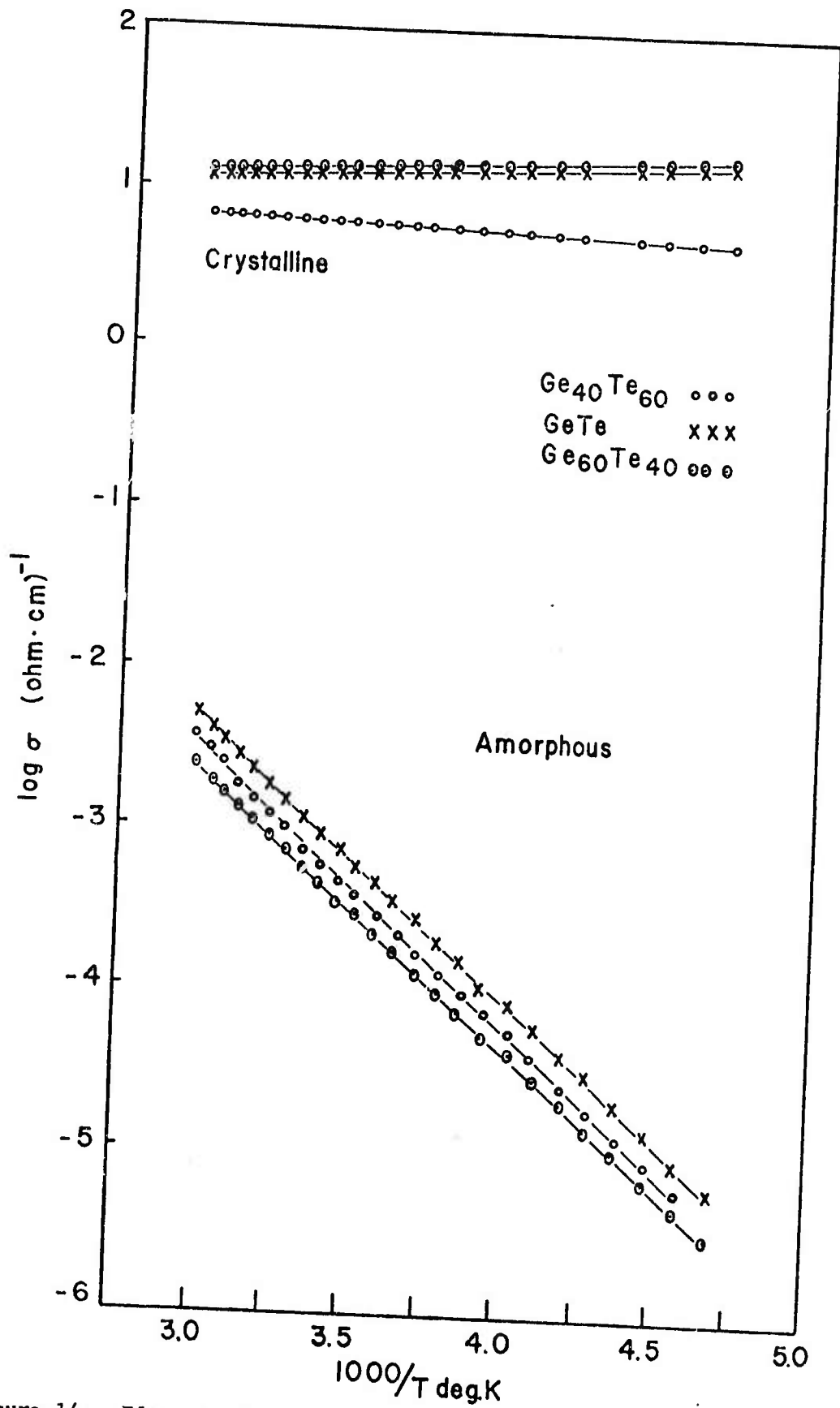
Figure 14. Electrical conductivity of Ge_xTe_{1-x} as a function of reciprocal temperature.
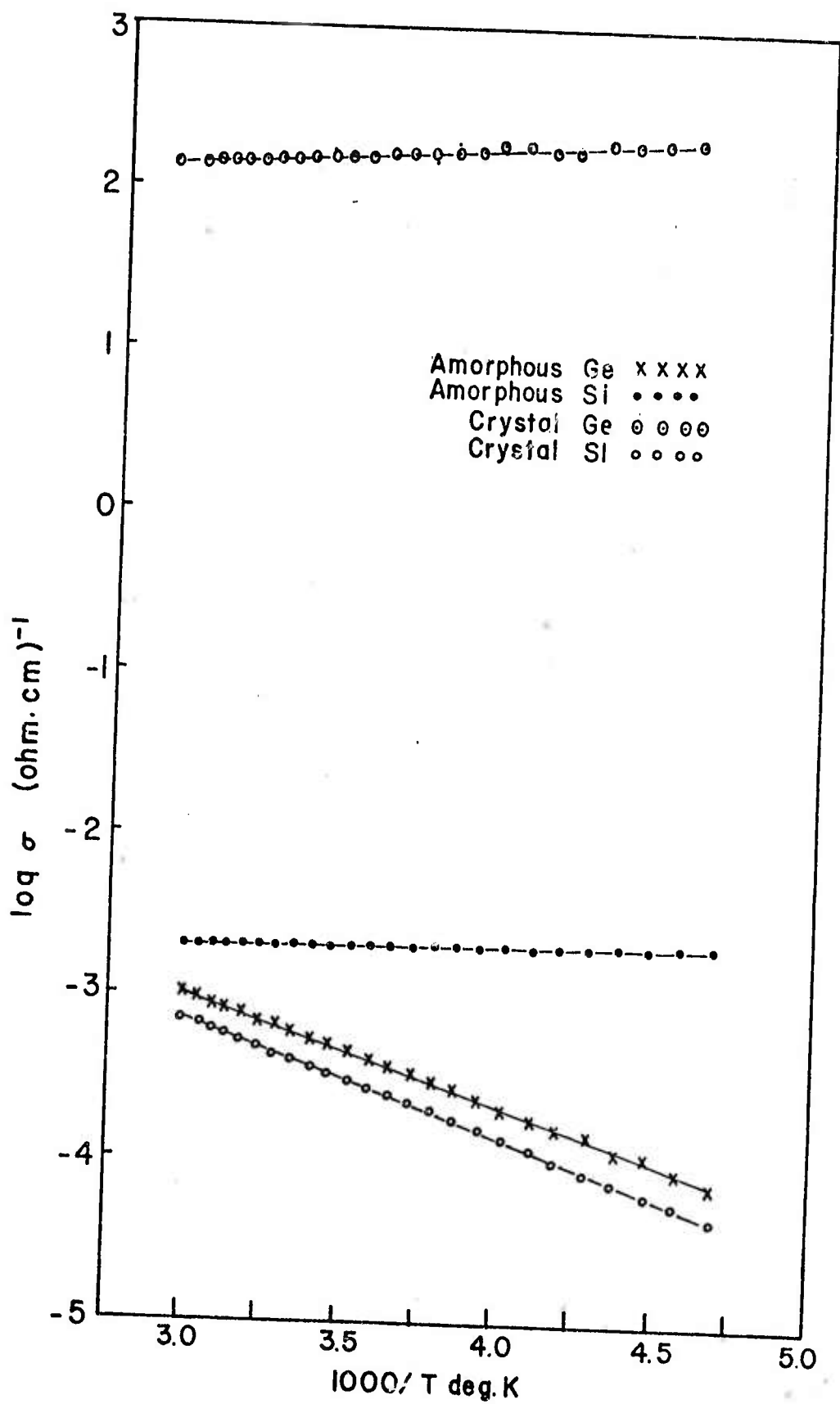
Figure 15.   Electrical conductivity of amorphous and crystalline germanium and silicon as a function of reciprocal temperature.

in electrical conductivity of amorphous films, relative to crystalline samples, Figure 13, since electron traps would tend to reduce carrier lifetimes and hence d.c. electrical conductivity.

The amorphous valence level spectra of Ge_xTe_{1-x} are very sharp and well defined while the crystalline valence electron levels are broad except for crystalline GeTe whose valence level spectrum shows a sharp, well defined peak. This result is expected since $Ge_{40}Te_{60}$ and $Ge_{60}Te_{40}$ are two phase alloys that contain GeTe + Ge and GeTe + Te respectively. The GeTe phase, occurring at 5.3 eV of binding energy, is manifest as a shoulder on the high energy side of the $Ge_{40}Te_{60}$ and $Ge_{60}Te_{40}$ valence level peaks. Coupled with the lack of significant shifts in subvalence levels, the above observations indicate that the bonding in Ge_xTe_{1-x} compositions is a mixture of covalent and metallic bonding and that at $x = 0.5$ bonding is principally covalent with an ionic component. The principle reason for the different bonding in GeTe is evident when the electronic configurations of Ge and Te are considered. Germanium has the electronic structure

$$1s^2 2s^2 2p^6 3s^2 3p^6 3d^{10} 4s^2 4p^2$$
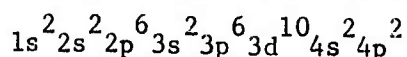
and tellurium has the electronic structure

$$1s^2 2s^2 2p^6 3s^2 3p^6 3d^{10} 4s^2 4p^6 4d^{10} 5s^2 5p^4$$
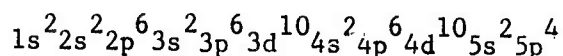
Thus Ge and Te complement each other so that there are just enough p level electrons to complete the outer band of one or other of the atoms. The electro-negativities of Ge and Te, 1,8 and 2.1 respectively, indicate that neither atom is sufficiently electronegative to ionize the other. The result being a covalent bond that is approximately 0.3% ionic.

Sharp valence electron peaks in amorphous films of Ge_xTe_{1-x} compositions, occur at approximately 3.4 eV of binding energy and indicate that the

structure of the amorphous films is nearly identical but different from the structure of crystalline materials of the same composition. The shift to lower binding energy of the main body of the valence level peak indicates that the band has become less ionic. A similar conclusion was reached by Betts, et. al.[25].

Spectral studies of Ge_xSe_{1-x} compositions show the same essential features as those of Ge_xTe_{1-x}. Broad valence bands characteristic of crystalline $GeSe_2$ and GeSe are the result of two phases. These valence level spectra appear to be a mixture of the valence levels of the elemental end members Ge and Se.

Amorphous $Ge_{43.5}Se_{56.5}$ has a valence level structure that is entirely different from the valence level structures of amorphous $GeSe_2$ and GeSe. The two s-like levels, located at 9.5 eV and 8.1 eV, probably arise due to the complete filling of the 4s levels of Ge and Se while the broad structure near the zero of binding energy is the result of partially filled 4p levels.

The very sharp valence level doublet in elemental selenium is suprising in terms of the amorphous films of Ge, Si and carbon. However, the structure of amorphous selenium is known to be polymer like octagonal rings.[26] Apparently the well defined molecular structure of amorphous Se is the result of strong covalent bands that retain sharp definition in the valence electron structure. A similar molecular approach would explain the sharp valence level structure seen in amorphous Ge_xTe_{1-x} and Ge_xSe_{1-x} alloys. Such a structural model, proposed by Bienenstack[25], suggests that amorphous films of GeS, GeSe and GeTe have a modified black phosphorous structure in which tetrahedral units are arranged in layered chains. The intrachain bonds are strong and covalent while interchain bonding is a weaker Van der Wall force.

Amorphous AsTe, like $Ge_{43.5}Se_{56.5}$, has S-like valence levels located at 10.0 eV and 8.5 eV. It is thought that these S-like levels are the result of completely filling the 4s levels, through a sharing of electrons. AsTe like GeTe and $Ge_{43.5}Se_{56.5}$ has an electronic structure that indicates that the atomic structure in the amorphous film is very different from the atomic structure of the crystal.

Summary

The spectroscopic data, summarized in Table I, coupled with electrical conductivity data, shows that the electrical behavior and electronic structure of amorphous films is very different from crystals of the same composition. The differences in electrical conductivity of the amorphous and crystalline forms of Ge and Si are related to structural defects while the changes in Ge_xTe_{1-x} and Ge_xSe_{1-x} alloys are the result of a different band type.

Figure	Composition	Observation
1	Ge	Sharp crystalline valence level and no amorphous valence level peak.
2	Ge	R.F. sputtered and vapor deposited films are identical.
3	Si	Sharp crystalline valence level with similar R.F. sputtered and vapor deposited amorphous valence levels.
4	C	Valence levels of an amorphous carbon film.
5	$Ge_{40}Te_{60}$	Broad crystalline valence levels with sharp amorphous valence levels.
6	GeTe	Sharp crystalline valence levels and sharp amorphous valence levels. Crystalline levels are shifted by 2.1 eV to higher binding energy.
7	$Ge_{60}Te_{40}$	Broad crystalline valence levels and sharp amorphous valence levels.
8	Te	Sharp crystalline valence levels.
9	$GeSe_2$	Broad crystalline valence levels and sharp amorphous valence levels.
10	$Ge_{43.5}Se_{56.5}$	Two overlapping crystalline valence levels with sharp amorphous valence levels containing three definable peaks.
11	GeSe	Broad crystalline valence levels and sharp amorphous valence levels.
12	Se	Sharp doublet in the valence band.
13	AsTe	Sharp crystalline valence level and an amorphous valence level containing one doublet and a diffuse peak.

Table I.   Summary of Spectroscopic Data

Part I.   References

1. H. H. Nester and W. D. Kingery, "Electrical Conduction in Vanadium Oxide Glasses," Proc. Seventh International Congress of Glass, Brussels, Gordon and Breach, New York, (1965).

2. J. E. Stanworth, E. P. Denton, and H. Rawson, "Vanadate Glasses," Nature, $\underline{173}$, 1030 (1954).

3. J. E. Stanworth, R. E. Baynton, and H. Rawson, "Semiconducting Properties of Some Vanadate Glasses," J. Electrochem. Soc., $\underline{104}$, 237 (1957).

4. J. E. Stanworth, E. P. Denton, and H. Rawson, "Vanadium Pentoxide Glasses with a Low Electrical Resistance," Chem. Abstr. $\underline{54}$, 17831i (1960).

5. R. H. Caley and M. Krishnamurthy, "Electrical Conductivity of Glasses in the System $P_4O_{10}-V_2O_5$ and $P_4O_{10}-WO_3$," J. Am. Ceram. Soc., $\underline{53}$, (5).

6. G. N. Greaves, "Small Polaron Conduction in $V_2O_5-P_2O_5$ Glasses," J. Non-crys. Solids, $\underline{11}$ (5), 427 (1973).

7. "Modern Aspects of the Vitreous State," Vol. 1, 2 & 3, edited by J. D. Mackenzie, Published by Butterworth, Inc., Washington, D. C. (1964).

8. M. Munakata, "Electrical Conductivity of High Vanadium Phosphate Glass," Solid State Electronics, $\underline{1}$, 159 (1960).

9. I. I. Kitaigorodskii and V. G. Karpechenko, "Synthesis and Investigation of Certain Vanadium Glasses," Stelko i Keram., $\underline{15}$, 8 (1958).

10. B. Nador, "Properties of Glasses of the System $V_2O_5-P_2O_5$," Stelko i Keram, $\underline{17}$, 18 (1960). Chem. Abstr. $\underline{55}$, 2045d (1961).

11. S. V. Poberovskenya, V. A. Ioffe, and I. V. Patrina, "Electrical Properties of Certain Semiconducting Oxide Glasses," Soviet Physics Solid State, $\underline{2}$, 609 (1966).

12. B.V.J. Rao, "Structure and Mechanism of Conduction of Semiconductor Glasses," J. Am. Ceram. Soc., $\underline{48}$ (6), 311 (1965).

13. M. Matsuoka, T. Masuyama and Y. Iida, "Nonlinear Electrical Properties of Zinc Oxide Ceramics," Japan J. Appl. Phys., Suppl. 39, 94-101 (1970).

14. M. Matsuoka, T. Masuyama, and Y. Iida, "Voltage Nonlinearity of Zinc Oxide Ceramics Doped with Alkali Earth Metal Oxide," Japan J. Appl. Phys., 8, 1275 (1969).

15. W. G. Morris, "Electrical Properties of $ZnO-Bi_2O_3$ Ceramics," J. Am. Ceram. Soc., 56 (7) 360-364 (1973).

16. E. M. Levin and R. S. Roth, J. Research Natl. Bur. Standards, 68A (2), 199 (1964).

17. R. W. Frankson and L. H. Slack, "Low Temperature Coefficients of Resistance in Manganese Oxide Films," accepted for publication in the Bull. Am. Ceram. Soc. (See also R. W. Frankson, "Temperature Independent Electrical Conduction in Some Oxide Thin Films," M.S. Thesis, Virginia Polytechnic Institute and State University (1970).)

18. T. M. Donovan, W. E. Spicer, J. M. Bennett, and E. J. Ashley, "Optical Properties of Amorphous Germanium Films," Physical Review B, 2, 2, p. 397-413 (1970).

19. M. L. Théye, "Influence of Annealing on the Optical Properties of Amorphous Germanium Films," Mat. Res. Bull., 6, p. 103-118 (1971).

20. Kai Siegbahn, Carl Nording, and Anders Fahlman, Electron Spectroscopy for Chemical Analysis. Technical Report AFML-TR-68-189.

21. D. A. Shirley, ed., Electron Spectroscopy, North-Holland Pub. Co. (1972).

22. L. B. Valdes, "Resistivity Measurements on Germanium for Transistors," Proc. of The Inst. of Radio Eng., 42, Jan-June 1954.

23. L. Ley, S. Kowalczyk, R. Pollak, and D. A. Shirley, "X-Ray Photoemission Spectra of Crystalline and Amorphous Si and Ge Valence Bands," Phys. Rev. Letters, 29, 16 (1972).

24. L. V. Azaroff and J. J. Brophy, Electronic Processes in Materials, McGraw-Hill (1963).

25. F. Betts and A. Bienenstock, "Structure and Bonding in Amorphous Ge_xTe_{1-x} Alloys," J. Non-Cryst. Solids, 8-10 (1972).

26. David Adler, "Amorphous Semiconductors," CRC Critical Reviews in Solid State Sciences (1971).

27. Arthur Bienenstock, "Threefold Coordination Model Structure of Amorphous GeS, GeSe and GeTe," J. Non-Cryst. Solids, 11, p. 447-458 (1973).